Georgopanos, P.; Handge, U.A.; Abetz, C.; Abetz, V.:

Influence of block sequence and molecular weight on morphological, rheological and dielectric properties of weakly and strongly segregated styrene-isoprene triblock copolymers

In: Polymer (2016) Elsevier

DOI: 10.1016/j.polymer.2016.02.039

Influence of block sequence and molecular weight on morphological, rheological and dielectric properties of weakly and strongly segregated styrene-isoprene triblock copolymers

Prokopios Georgopanos[1], Ulrich A. Handge[1], Clarissa Abetz[1], Volker Abetz[1,2]*

[1]*Institute of Polymer Research, Helmholtz-Zentrum Geesthacht, Max-Planck-Str. 1, 21502 Geesthacht, Germany*
[2]*Institute of Physical Chemistry, University of Hamburg, Martin-Luther-King-Platz 6, 20146 Hamburg, Germany*

* *Volker Abetz (Corresponding author)*
e-mail: volker.abetz@hzg.de, Tel: +49 4152 87 2461, Fax: +49 4152 87 2499

In memoriam Dr. rer. nat. habil. Víctor Hugo Rolón Garrido

Abstract

In this work, morphological, thermal, viscoelastic and dielectric properties of triblock copolymers consisting of styrene (S) and isoprene (I) blocks are discussed. SIS and ISI triblock copolymers were synthesized by sequential anionic polymerization, three of them exhibiting molecular weights below the entanglement molecular weight M_e, three of them exhibiting molecular weights in the order of M_e and two of them exhibiting molecular weights above M_e. The objective of this work is the investigation of the influence of molecular weight and block sequence on relaxation of the block copolymer chains. Morphological investigations using small angle X-ray scattering and transmission electron microscopy studies reveal that a larger molecular weight is associated with a more pronounced microphase separation. The presence of two glass transition temperatures reveals microphase separation of the PI and PS blocks. The Fox-Flory equation was applied in order to describe the molecular weight dependence of the glass transition temperature of the polyisoprene and the polystyrene blocks. The analysis of rheological data reveals a Maxwell fluid behaviour for the weakly segregated block copolymers, whereas for the strongly segregated block copolymers a pronounced elastic behaviour at low frequencies of small amplitude shear oscillations was observed. In the intermediate regime of molecular weight, a complex viscoelastic behaviour appears. The plateau modulus G_N^0 is influenced by the sequence of the PS and the PI blocks (SIS or ISI). Our analysis of segmental and normal mode relaxation in dielectric spectroscopy experiments show that the relaxation processes are strongly influenced by the block sequence (PI blocks tethered at one or

both ends) and the molecular weight. As a result, the block sequence in triblock copolymers influences dynamical properties in the glassy state and in the melt.

Keywords: Triblock copolymers, morphology, rheology, dielectric spectroscopy, glass transition

1. Introduction

Block copolymers are materials known since many decades. A huge variety of block copolymers exists due to many possible combinations of different blocks, accessible by an increasing number of different synthetic methods [1-4]. They exhibit particular properties which are caused by the combination of different blocks most often leading to self-assembled periodic microphase separated structures. The application of block copolymers in modern material science varies from blends [5-12], nanopatterning [13-18] to membranes [19-27].

Commercially well-known block copolymers are AB multiblock copolymers of hard and soft blocks, where the hard blocks are often a polyamide or a polyester, and the soft blocks are a polyether like poly(ethylene glycol) [26, 27]. The simplest multiblock copolymers are linear triblock copolymers. This type of polymers consists of three blocks which can differ from each other (ABC) [28-37] or can have two similar blocks (ABA) [37-43]. Numerous studies on synthesis of triblock copolymers via anionic as well as controlled radical polymerization have been published. In the review of Matsuo et al. [44] the recent advances in synthesis of ABC and ABA triblock copolymers via anionic polymerization are presented. Davis et al. [45] give details on the synthesis of ABC triblock copolymers via atom transfer radical polymerization, while Agudelo et al. [46] describe the synthesis of ABA triblock copolymers via controlled atom transfer radical polymerization. The presence of the third block changes the properties enabling further applications, e.g., the use of thermoplastic elastomers such as polystyrene-*b*-polybutadiene-*b*-polystyrene and polystyrene-*b*-polyisoprene-*b*-polystyrene triblock copolymers as additive in oils and asphalt, in automotive industry, as adhesives, or in medical applications, etc. [47].

Matsen presented a theoretical approach on the microphase separation of symmetric and asymmetric ABA triblock copolymers, indicating that the symmetry of the relative composition of the two outer blocks and the total composition play a very important role on the morphology [48, 49]. Alig et al. [50] described the rheological and dielectric properties of a similar triblock copolymer. In their study, lamellar SIS triblock copolymers were synthesized via sequential anionic polymerization. The analysis of their dielectric experiments indicates that the normal mode relaxation of the PI block is associated with the junction point fluctuations. Using the dielectric data, Alig et al. also estimated the interfacial thickness of the lamellar microstructure. Furthermore, low molecular weight SIS triblock copolymers and the SI diblock copolymer precursor were examined by Watanabe et al. [51, 52] using

dielectric spectroscopy and small amplitude shear oscillations. The synthesis was carried out via anionic polymerization of the styrene and the isoprene monomers in order to synthesize in a first step a PS-*b*-PI diblock copolymer precursor. Then the triblock copolymer was obtained by coupling reaction of the living diblock copolymer precursor with *p*-xylene dichloride. The effect of loop and bridge formation of the middle block on the relaxation of the polymer was thoroughly examined. Polystyrene-*b*-polyisoprene star block copolymers were studied by Floudas et al. [53]. The authors concluded that the macromolecular architecture influences the chain dynamics through the localization of the star center (junction point of the diblock copolymer arms). Investigations on the alignment of lamellar forming SI block copolymers with a heptablock architecture (SISISIS) was also performed [54] and the role of chain confirmation (bridge to loop transition) was elucidated. Recently, dielectric spectroscopy studies on polystyrene-*b*-polyisoprene diblock copolymers with a high polyisoprene content under nanoconfinement were performed and combined Havriliak-Negami fits in the frequency and temperature domain were carried out [55, 56]. The studies revealed that the nanoconfinement did not influence the segmental mode relaxation of the two different blocks, nevertheless the normal mode relaxation of the polyisoprene block was significantly affected.

In this work, the properties of styrene-isoprene triblock copolymers exhibiting different block sequences and molecular weights are studied. Triblock copolymers of polystyrene-*b*-polyisoprene-*b*-polystyrene (SIS) and polyisoprene-*b*-polystyrene-*b*-polyisoprene (ISI) triblock copolymers were synthesized via anionic polymerization. In all cases the samples were prepared sequentially without the use of any type of linking agent. In contrast to the majority of previous works where polystyrene formed the minority component, the polyisoprene content was kept at approximately 20 wt%. The polymers were characterized to determine their molecular, morphological and thermal properties. Broadband dielectric spectroscopy and rheological experiments in the melt state allow for analyzing relaxation phenomena on different time scales. Through linear viscoelastic shear oscillations in the melt and broadband dielectric spectroscopy the effect of the molecular weight and the block sequence on the dynamical properties of the copolymers was investigated, in particular the behaviour of the short polyisoprene block in the middle (SIS) of the block copolymer or at its chain ends (ISI). Morphological characterization was accomplished by transmission electron microscopy (TEM) and small angle X-ray scattering (SAXS).

2. Experimental section

2.1 Materials

Styrene (Sigma-Aldrich, Schnelldorf, Germany, 99%) was purified from aluminum oxide (Macherey-Nagel, Düren, Germany) and subsequently distilled from di-*n*-butylmagnesium (Sigma-Aldrich, Schnelldorf, 1.0 M solution in heptane) under high vacuum. Isoprene (Sigma-Aldrich, Schnelldorf, Germany, 99%) was purified from calcium hydride (Sigma-Aldrich, Schnelldorf, Germany, >90%) and twice from *n*-butyllithium (*n*-BuLi, Sigma-Aldrich, Schnelldorf, Germany, 1.6 M solution in hexane). The solvent used was cyclohexane (Merck, Germany, 99.5%), distilled from calcium hydride in a glass flask with $PS^{(-)}Li^{(+)}$. As initiator, *sec*-butyllithium (*sec*-BuLi, Sigma-Aldrich, Schnelldorf, Germany, 1.4 M solution in cyclohexane) was used. As termination agent a 10:1 mixture of methanol (Sigma-Aldrich, Schnelldorf, Germany, 99.8%) and acetic acid (Sigma-Aldrich, Schnelldorf, Germany, 99.7%) was used.

2.2 Instrumentation

GPC measurements were performed at room temperature in THF on a Waters instrument (Waters GmbH, Eschborn, Germany), equipped with polystyrene gel columns of 10, 10^2, 10^3, 10^4 and 10^5 Å pore sizes, using a refractive index (RI) detector. Polystyrene and 1,4-polyisoprene polymer standards of different molecular weights (Polymer Labs GmbH) were used. ^{1}H-NMR was accomplished with the Avance AVIII HD 500 MHz spectrometer (Bruker Biospin, Rheinstetten, Germany), equipped with a 500 MHz magnet and a triple resonance inverse (TXI) probe. The experiment was done at room temperature with deuterated chloroform as solvent and tetramethylsilane as internal standard.

Thermal characterization was accomplished via differential scanning calorimetry on bulk triblock copolymers using a calorimeter DSC 1 (Mettler-Toledo, Greifensee, Switzerland). The temperature range of the experiments was −100 °C up to +150 °C under argon atmosphere. A heating and cooling rate of 10 K/min was used. The second heating interval was analyzed for the determination of the glass transition temperature.

Rheological experiments in oscillatory mode were carried out using a rotational rheometer MCR 502 (Anton Paar GmbH, Graz, Austria). Cylindrical specimens with a diameter of 8 mm and a thickness

of 2 mm were prepared. Initially the bulk polymer powder was dried under vacuum overnight. Then the sample was compression molded at 135 ^{o}C for approximately 7 min, applying a force of approximately 60 kN and vacuum (pressure of 10^{-5} bar). It should be mentioned at this point that the low molecular weight triblock copolymer samples were very brittle due to the low molecular weight (the molecular weight of both blocks are below the entanglement molecular weight of the respective homopolymers) and the high weight fraction of polystyrene. A parallel plate geometry tool for 8 mm cylindrical specimens was used and the gap for the measurements was set to 1.95 mm. The melting - annealing time was 7 min.

Several types of rheological experiments were performed. In order to test the thermal stability of the materials under investigation, time sweeps at an angular frequency of ω = 0.10 rad s^{-1} with a shear amplitude of 5% were performed at selected temperatures. Frequency sweeps were performed in the frequency range ω = 100 – 0.01 rad s^{-1} at a shear amplitude of 5%. The frequency sweeps were started at the highest frequency. Temperature ramps were also performed at an angular frequency of ω = 0.10 rad s^{-1}. The shear amplitude was 5%, and a specific temperature interval (from the melt to the glassy state of polystyrene) was selected depending on the polymer. The highest temperature was the start temperature. The cooling rate was 0.5 K/min.

Dielectric spectroscopy measurements were performed using an Alpha-AN high resolution dielectric analyzer (Novocontrol Technologies GmbH, Montabaur, Germany). Films were directly cast on a brass, gold coated cylindrical plate from solution in chloroform, leading to films of approximately 80 - 100 μm thickness, after drying in air at room temperature over a period of two days. Then the samples were annealed under vacuum overnight at 130 ^{o}C. A second brass plate was placed on top of the sample. Afterwards the two brass plates containing the sample were inserted into the spectrometer. Before the measurement the sample was heated up to a temperature approximately 15 ^{o}C above the glass transition temperature of the polystyrene block for one hour in order to achieve good adhesion of the sample with the electrodes. A good adhesion of the sample is of great importance for the dielectric spectroscopy measurement since due to the polystyrene majority the sample tends to detach from the metal plate. Selected experiments without the annealing procedure were also performed. The diameter of the brass plates was 40 mm. Isothermal frequency sweeps experiments were accomplished from -80 ^{o}C to 150 ^{o}C with an increment of 4 ^{o}C in a range of 10^{-3} to 10^{6} Hz, starting with the highest frequency and a stabilization time of 120 s. Additionally temperature

ramp experiments of non-annealed samples were accomplished at the same temperature range with an increment of 2 °C and a measurement frequency of 10 Hz.

Transmission electron microscopy (TEM) investigations were done using a Tecnai G^2 F20 electron microscope (FEI, Eindhoven, The Netherlands), operated at 120 kV, in the bright field mode. Compression molded samples and polymer films were examined to achieve morphological information in order to correlate the results from rheological and dielectric measurements. Polymer films were cast from chloroform solutions and slowly dried in presence of solvent vapor in a desiccator for a time period of approximately 10 days. Chloroform was chosen as solvent for this triblock copolymer system to allow a direct comparison with the samples used in broadband dielectric spectroscopy experiments. The dried films were annealed at 135 °C for several hours under vacuum. Ultra-thin sections of about 50 nm were cut at -150 °C with a Leica Ultramicrotome EM UCT (Leica Microsystems, Wetzlar, Germany) equipped with a diamond knife. In order to increase the electron density contrast, the polyisoprene block was selectively stained by exposure to OsO_4 vapor.

Small angle X-ray scattering (SAXS) experiments were performed at Beamline P12 of Petra III synchrotron storage ring at DESY in Hamburg, Germany. A Pilatus 2M detector was used at a distance of 4.1 m. The exposure time was 0.045 s and the exposure period 0.05 s. A total number of 20 frames was acquired per measurement. The beam size was 0.1 x 0.2 mm^2 and the energy was 10 keV. For the SAXS experiments parts of the unstained films prepared for the TEM experiments were used as well as compression molded samples. The scattering intensity I was analyzed as a function of the scattering vector q which is given by:

$$q = (4\pi/\lambda)\cdot\sin\theta \qquad (1)$$

with θ being half of the scattering angle and λ the wavelength of X-ray radiation.

2.3 Synthesis of triblock copolymers

The SIS triblock copolymers were synthesized via sequential anionic polymerization. The synthesis started with the polymerization of styrene using *sec*-BuLi as initiator, in cyclohexane at room temperature (RT) for 24 h. Following that, a small aliquot was removed from the polymerization

reactor and terminated with degassed methanol for molecular characterization of the first block. Afterwards, the purified isoprene was added to the mixture and let to react for 24 h. Again a small aliquot was taken in order to verify the polymerization of the isoprene and reveal the molecular characteristics of the polystyrene-*b*-polyisoprene (SI) precursor diblock copolymer. The last step was the addition of the styrene monomer for the synthesis of the third block. During the three polymerization propagation phases, characteristic colors indicated the livingness of the corresponding active chain end. In case of the low molecular weight triblock copolymers the polystyrene first block in cyclohexane showed a deep orange-red color. The addition of isoprene changed gradually the solution to light yellow. During the polymerization of the last polystyrene block again a deep orange color was observed. In case of the higher molecular weight triblock copolymer, due to the low concentration of the anionic living ends the colors were yellow for the first block, gradually colorless during the polymerization of the second block and again yellow during the synthesis of the final block. The last step for the synthesis was the controlled termination of the polymerization with a mixture of degassed methanol and acetic acid. At this step the color of the polymerization solution disappeared immediately afterwards. The polymer was precipitated in cold methanol. Finally, the sample was dried and kept in vacuum at 30 ^{o}C. The synthesis process is presented in **Scheme 1(a)**.

The synthesis of the ISI triblock copolymers was performed in a similar way to the synthesis of the SIS triblock copolymers. In this case the polymerization started with the polymerization of isoprene using *sec*-BuLi. Following, polymerization of styrene took place and the last step was the addition of the isoprene for the synthesis of the third block. The solution of the polyisoprene first block in cyclohexane was colorless. The addition of styrene turned the solution into orange color in case of the low molecular weight and into yellow in case of the higher molecular weights while the addition of the last polystyrene block the color disappeared gradually, but remained slightly yellow in case of the low molecular weight or disappeared gradually until no color indication in case of the high molecular weight. The termination, precipitation, sample drying and storage was the same alike the SIS triblock copolymers. The synthesis process is presented in **Scheme 1(b)**.

The nomenclature given to the synthesized samples is $S_yI_xS_z^M$ or $I_yS_xI_z^M$ where x,y,z are the weight percentages of the corresponding blocks and M is the number averaged molecular weight of the block copolymer in kg/mol.

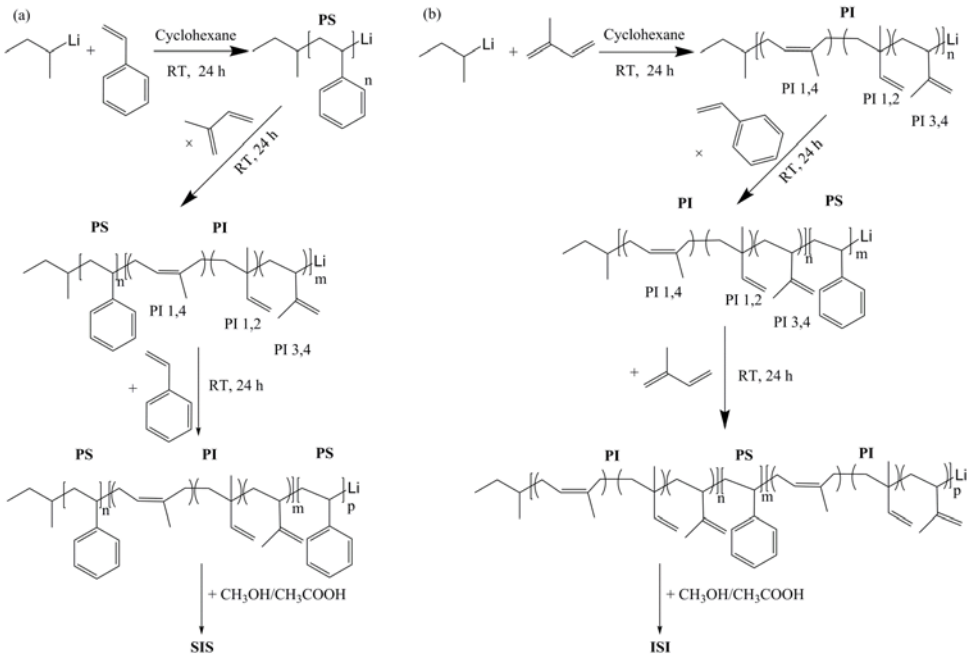

Scheme 1. Synthesis scheme for (a) SIS and (b) ISI triblock copolymers via sequential anionic polymerization.

3. Results and discussion

3.1 Molecular characterization

The triblock copolymers were characterized by means of gel permeation chromatography and proton nuclear magnetic resonance spectroscopy. The analysis of the molecular composition was based on the combination of these two methods. Eight triblock copolymers were synthesized. The results are summarized in Table 1(a) for the SIS and in Table 1(b) for the ISI triblock copolymers. The entanglement molecular weights of polystyrene and polyisopene are 18 700 g/mol [57] and 6 400 g/mol [58], respectively. The data in Table 1 shows that three triblock copolymers ($S_{39}I_{22}S_{39}^{11}$, $S_{30}I_{28}S_{42}^{16}$ and $I_9S_{82}I_9^{17}$) are below the entanglement molecular weights of PS and PI. Two triblock copolymers ($S_{35}I_{23}S_{42}^{161}$ and $I_8S_{78}I_{14}^{98}$) are clearly above the entanglement molecular weights of PS

and PI. The molecular weight of the other three triblock copolymers ($S_{43}I_{20}S_{37}^{57}$, $I_{15}S_{73}I_{12}^{35}$ and $I_{10}S_{83}I_{7}^{67}$) belongs to an intermediate range of molecular weight where only an onset of ($I_{15}S_{73}I_{12}^{35}$) or a partial entanglement network ($S_{43}I_{20}S_{37}^{57}$ and $I_{10}S_{83}I_{7}^{67}$) exists. Microphase separation of block copolymers is determined by the value of χN where χ is the Flory-Huggins interaction parameter for the pair polystyrene/1,4 - polyisoprene and *N* is the total degree of polymerization. The value of χN is in the order of 15 for triblock copolymers with a total molecular weight being equal to the entanglement molecular weight. Consequently, the onset of entanglement effects and microphase separation appears for a similar range of molecular weight in these materials.

Table 1. Molecular characteristics based on GPC and ^{1}H-NMR measurements of the (a) SIS and (b) ISI triblock copolymers.

(a)

SIS [a]	$\bar{\mathbf{M}}_{\mathbf{n}}^{\mathbf{PS}}$ [b] (g/mol)	$\bar{\mathbf{M}}_{\mathbf{n}}^{\mathbf{PI}}$ [b] (g/mol)	$\bar{\mathbf{M}}_{\mathbf{n}}^{\mathbf{PS'}}$ [b] (g/mol)	$\bar{\mathbf{M}}_{\mathbf{n}}^{\mathbf{SIS}}$ [b] (g/mol)	f^{PS} [d] (wt%)	f^{PI} [d] (wt%)	χN [e]	PDI [b]
$S_{39}I_{22}S_{39}^{11}$	4 000	3 000	4 100	11 000	78	22	10.7	1.08
$S_{30}I_{28}S_{42}^{16}$	4 600	5 200	6 200	16 000	72	28	16.0	1.09
$S_{43}I_{20}S_{37}^{57}$	26 000	13 500	17 000	56 500	80	20	54.4	1.07
$S_{35}I_{23}S_{42}^{161}$	51 800	45 700	63 600	161 000	77	23	158.6	1.20

(b)

ISI	$\bar{\mathbf{M}}_{\mathbf{n}}^{\mathbf{PI}}$ [c] (g/mol)	$\bar{\mathbf{M}}_{\mathbf{n}}^{\mathbf{PS}}$ [c] (g/mol)	$\bar{\mathbf{M}}_{\mathbf{n}}^{\mathbf{PI'}}$ [c] (g/mol)	$\bar{\mathbf{M}}_{\mathbf{n}}^{\mathbf{ISI}}$ [c] (g/mol)	f^{PS} [d] (wt%)	f^{PI} [d] (wt%)	χN [e]	PDI [c]
$I_9S_{82}I_9^{17}$	1 600	12 600	2 400	17 000	82	18	15.9	1.03
$I_{15}S_{73}I_{12}^{35}$	4 600	28 900	5 600	35 000	73	27	34.2	1.08
$I_{10}S_{83}I_7^{67}$	7 400	51 700	7 400	67 000	83	17	63.7	1.02
$I_8S_{78}I_{14}^{98}$	7 200	79 400	18 300	98 000	78	22	95.2	1.10

[a] Lower case numbers indicate the mass fraction of the corresponding block in wt%, the upper case number indicates the total number averaged molecular weight in kg/mol.
[b] Determined from GPC calibrated with polystyrene standards and ^{1}H-NMR
[c] Calculated from GPC calibrated with 1,4-polyisoprene standards and ^{1}H-NMR
[d] Calculated from ^{1}H-NMR
[e] Calculated using the total degree of polymerization *N* of the triblock copolymer and the Flory-Huggins interaction parameter χ = 0.089 (at 135 ^{o}C) [59]

3.2 Thermal analysis

The glass transition temperature of the polystyrene and the polyisoprene blocks of the triblock copolymers depend on the molecular weight of the two blocks and the degree of segregation (complete miscibility, weak/strong segregation). **Fig. 1** presents the thermograms of the second heating interval. The values of the glass transition temperatures are listed in **Table 2**. In case of the SIS triblock copolymers, the triblock copolymer with the lowest molecular weight ($S_{39}I_{22}S_{39}^{11}$) only shows a single glass transition resulting from the complete miscibility of the polystyrene and the polyisoprene blocks. The triblock copolymer $S_{30}I_{28}S_{42}^{16}$ exhibits a glass transition at approximately -50 °C corresponding to the PI block and a glass transition at approximately 43 °C corresponding to the PS block. These glass transition temperatures indicate partial mixing (weak segregation) of the two microphases as also reported for diblock copolymers in a similar range of molecular weights [60]. On the contrary, the higher molecular weight SIS triblock copolymers exhibit a glass transition temperature at approximately -65 °C for the PI block and at around 100 °C for the PS block. No intermediate glass transition temperature is visible because of the strong segregation of the two microphases. In case of the ISI triblock copolymers similar results for the thermal transitions were obtained. The triblock copolymer $I_9S_{82}I_9^{17}$ only shows a single glass transition because of complete miscibility of the polystyrene and the polyisoprene blocks. For the triblock copolymer $I_{15}S_{73}I_{12}^{35}$ with a molecular weight of 35 kg/mol the glass transition temperature of the PI block is -65 °C and the glass transition of the PS block is approximately 74 °C. The two higher molecular weight ISI triblock copolymers belong to the strongly segregated regime and are associated with a PI glass transition at -70 °C and a PS glass transition at around 94 °C. In summary, the DSC data show clear trends in the glass transition temperature. A larger total molecular weight yields a more pronounced microphase separation and thus a larger difference of the glass transition temperatures of the PS and the PI blocks up to the limiting T_g values of the corresponding homopolymers for infinite molecular weights. The degree of segregation which depends on the molecular weight strongly influences the thermal transition of both types of blocks. The presence of two different glass transitions for six triblock copolymers of this study reveals that at least a weak segregation has been achieved.

The Fox-Flory model for completely miscible polymers was applied to the weakly microphase-segregated triblock copolymers in order to calculate the fraction of PS and PI blocks in the partially

mixed microphases. The glass transition temperature T_g which results from the complete mixing of the PS and the PI blocks with weight fractions f^{PS} and f^{PI} is given by

$$\frac{1}{T_g} = \frac{f^{PS}}{T_g^{PS}} + \frac{f^{PI}}{T_g^{PI}} \quad (2)$$

Furthermore, the fractions of the PS and the PI blocks in the mixed microphases are related by

$$f^{PI} = 1 - f^{PS} \quad (3)$$

Equations (2) and (3) hold for both microphases. In this work the Fox-Flory equation was used in order to estimate the weight fraction of the two blocks in the mixed sections. In Table 2 the calculated weight fractions of the two blocks in the polyisoprene and polystyrene rich domains are listed. The values of T_g^{PS} and T_g^{PI} in Eq. (2) were calculated using the Bicerano equation

$$T_g = T_{g,\infty} - 0.002715 \frac{{T_{g,\infty}}^3}{M_n} \quad (4)$$

taking into account the dependency of the glass transition temperature (in K) on the molecular weight (in g/mol in Eq. (4)) [61, 62]. The value of $T_{g,\infty}^{PS}$ is 106 °C (379.15 K) and the one of $T_{g,\infty}^{PI}$ is -63 °C (210.15 K) according to literature [63]. For the $S_{39}I_{22}S_{39}$[11], $S_{30}I_{28}S_{42}$[16] and $I_9S_{82}I_9$[17] triblock copolymers the PS rich microphase was mixed with approximately 22%, 16% and 15% PI while for the $I_{15}S_{73}I_{12}$[35] triblock copolymer the PS microphase was mixed with approximately 9% PI. The penetration of the PS block into the PI rich microphase in case of the $S_{30}I_{28}S_{42}$[16] triblock copolymer was approximately 21%, while only 3% for the $I_{15}S_{73}I_{12}$[35] triblock copolymer. The increase of the molecular weight yields a decrease of mixing of the two components. The validity of our approach was checked by comparing the theoretical and experimental total weight fractions of the PI microphase. The calculated total weight fraction of polyisoprene is larger than the one provided by NMR analysis which shows that the approach based on the Fox-Flory and the Bicerano equations underestimates the influence of polyisoprene on the glass transition (i.e. leads to too large values of the polyisoprene fraction).

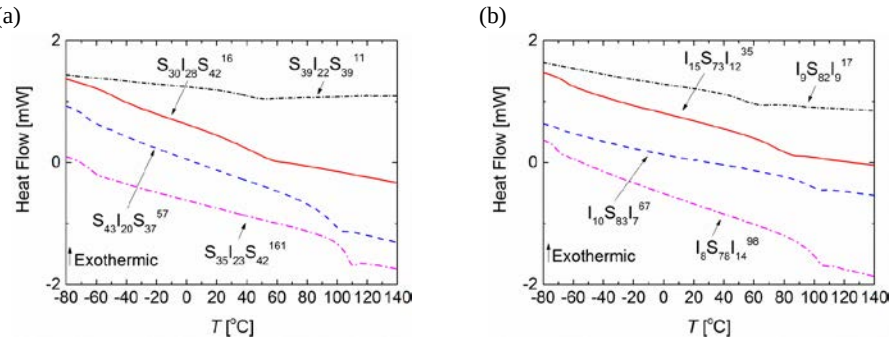

Fig. 1. DSC thermograms of (a) SIS and (b) ISI triblock copolymers. The curves are shifted vertically for clarity. The heating rate was 10 K/min.

Table 2. Thermal properties and mixing fractions of the PS and PI blocks in case of the low molecular weight triblock copolymers of (a) SIS and (b) ISI triblock copolymers.

(a)

SIS	T_g^{PI} [a] (°C)	T_g^{PS} [a] (°C)	T_g^{PI} [b] (°C)	T_g^{PS} [b] (°C)	PI rich microphase		PS rich microphase		f^{PI} [d]	f^{PS} [d]
					f^{PI} [c]	f^{PS} [c]	f^{PI} [c]	f^{PS} [c]		
$S_{39}I_{22}S_{39}^{11}$	-	38	-64	88	-	-	0.22	0.78	-	-
$S_{30}I_{28}S_{42}^{16}$	-48	43	-68	92	0.79	0.21	0.16	0.84	0.34	0.66
$S_{43}I_{20}S_{37}^{57}$	-67	96	-	-	-	-	-	-	-	-
$S_{35}I_{23}S_{42}^{161}$	-64	105	-	-	-	-	-	-	-	-

(b)

ISI	T_g^{PI} [a] (°C)	T_g^{PS} [a] (°C)	T_g^{PI} [b] (°C)	T_g^{PS} [b] (°C)	PI rich microphase		PS rich microphase		f^{PI} [d]	f^{PS} [d]
					f^{PI} [c]	f^{PS} [c]	f^{PI} [c]	f^{PS} [c]		
$I_9S_{82}I_9^{17}$	-	52	-69	94	-	-	0.15	0.85	-	-
$I_{15}S_{73}I_{12}^{35}$	-65	74	-66	101	0.97	0.03	0.09	0.91	0.33	0.67
$I_{10}S_{83}I_7^{67}$	-70	94	-	-	-	-	-	-	-	-
$I_8S_{78}I_{14}^{98}$	-72	98	-	-	-	-	-	-	-	-

[a] Determined from DSC experiments [b] Determined from Eq. (4) with use of T_g^{PS} = 106 °C and T_g^{PI} = -63 °C [63] [c] Calculated weight fractions of PI and PS, respectively, in each microphase. [d] Total concentration of PI and PS, respectively, calculated by adding the calculated weight fractions of PI and PS, respectively, in the two microphases based on Eq. (2).

3.3 SAXS analysis

In **Fig. 2** the results of SAXS experiments using thin films and compression molded samples are presented. In case of the compression molded samples the results (dashed lines) do not indicate a long range order of the microphase separated morphology. The scattering peaks cannot be clearly identified because the preparation method does not provide enough time for the sample to relax into complete equilibrium (completely long range ordered structure). On the contrary, the scattering curves corresponding to the thin films of the triblock copolymers (compact lines) indicate a more developed long range order. The morphology that is identified for the samples $S_{43}I_{20}S_{37}^{57}$, $S_{35}I_{23}S_{42}^{161}$ and $I_8S_{78}I_{14}^{98}$ according to the q^*/q_1 ratio is the morphology of hexagonally packed cylinders (polyisoprene cylinders in a polystyrene matrix). Here q^* denotes the magnitude of the scattering vector of the scattering peak and q_1 the magnitude of the scattering vector of the first scattering peak. The sample $I_{10}S_{83}I_7^{67}$ is associated with a spherical morphology, nevertheless only the characteristic peaks $1 : \sqrt{3} : \sqrt{6}$ are visible. The calculated q^*/q_1 ratios are indicated in the scattering diagram. The q ratios are in agreement with the International Tables of Crystallography and previous works [64, 65]. The films of the samples $S_{39}I_{22}S_{39}^{11}$, $S_{30}I_{28}S_{42}^{16}$, $I_9S_{82}I_9^{17}$, $I_{15}S_{73}I_{12}^{35}$ triblock copolymers do not indicated long range order (see supporting information, Fig. S1).

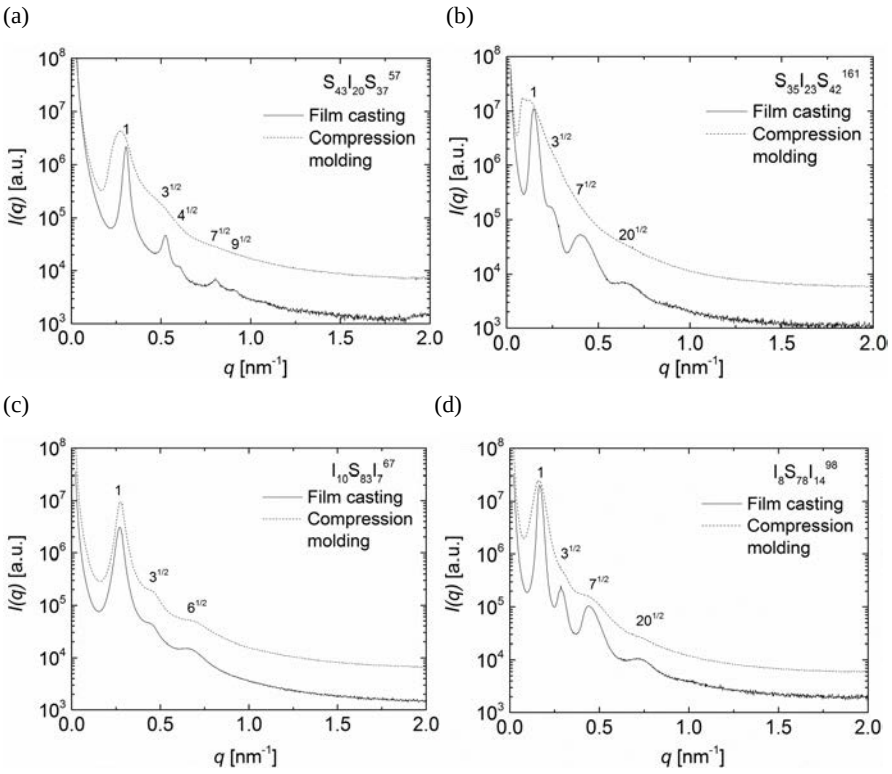

Fig. 2. Intensity *I* measured in SAXS experiments using films and compression molded samples as a function of the magnitude *q* of the scattering vector for the (a) $S_{43}I_{20}S_{37}^{57}$, (b) $S_{35}I_{23}S_{42}^{161}$, (c) $I_{10}S_{83}I_7^{67}$ and (d) $I_8S_{78}I_{14}^{98}$ triblock copolymers.

3.4 TEM analysis

Fig. 3 shows the transmission electron micrographs of the microphase separated $S_{43}I_{20}S_{37}^{57}$, $S_{35}I_{23}S_{42}^{161}$, $I_{10}S_{83}I_7^{67}$ and $I_8S_{78}I_{14}^{98}$ triblock copolymers which have been prepared by casting from solution in chloroform. The solvent was evaporated slowly over several days and finally the films were annealed under vacuum at 135 ºC. In solution, the average relaxation time of the polymer chains generally is much smaller than in the melt state. Consequently, a long-range order is achieved more rapidly for the triblock copolymer films than for the compression-moulded samples. With the

exception of the $I_{10}S_{83}I_7^{67}$ triblock copolymer, which shows PI spheres in a PS matrix, all other triblock copolymers show hexagonally packed PI cylinders in a PS matrix.

In case of the compression moulded samples (**Fig. 4**), the TEM investigations show similar microphase separated morphologies. However, because of the processing history, they are associated with a less pronounced long range order. The results of TEM investigations are in agreement with the SAXS data (**Fig. 2**), previous investigations and the theoretically calculated phase diagram for triblock copolymers [49, 66].

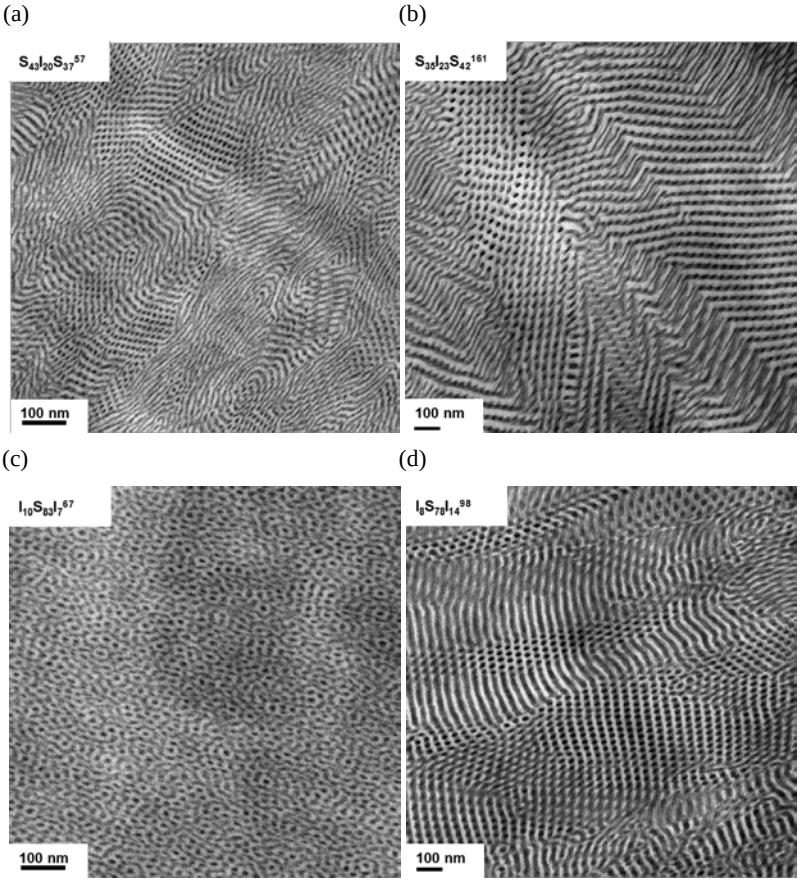

Fig. 3. Transmission electron micrographs of films of the triblock copolymers (a) $S_{43}I_{20}S_{37}^{57}$, (b) $S_{35}I_{23}S_{42}^{161}$, (c) $I_{10}S_{83}I_7^{67}$ and (d) $I_8S_{78}I_{14}^{98}$.

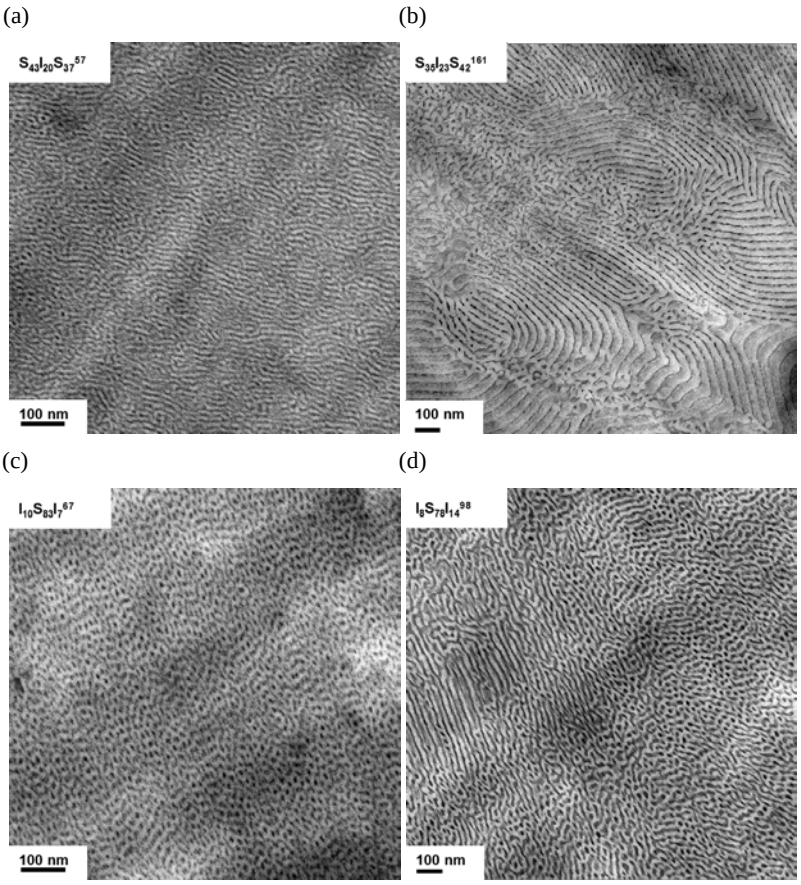

Fig. 4. Transmission electron micrographs of compression molded samples of the triblock copolymers (a) $S_{43}I_{20}S_{37}^{57}$, (b) $S_{35}I_{23}S_{42}^{161}$, (c) $I_{10}S_{83}I_7^{67}$ and (d) $I_8S_{78}I_{14}^{98}$.

3.5 Rheological analysis

Rheological experiments in the melt state generally allow for probing the relaxation behaviour of polymer chains at larger time scales than in dielectric experiments. In a first step, the thermal stability of the materials was investigated. The thermal stability of block copolymers can be influenced by chemical reactions (degradation or chemical crosslinking) and morphological changes. A time-sweep

experiment of a pristine polyisoprene homopolymer (not shown) at a temperature of 240 and 300 °C revealed that chemical crosslinking of polyisoprene can be excluded in the presence of a nitrogen atmosphere, see Ref. [67]. The dynamic moduli measured in frequency and time-sweeps of the three triblock copolymers with the lowest ($S_{39}I_{22}S_{39}^{11}$, $S_{30}I_{28}S_{42}^{16}$, $I_9S_{82}I_9^{17}$) and of the two triblock copolymers ($S_{35}I_{23}S_{42}^{161}$, $I_8S_{78}I_{14}^{98}$) with the highest molecular weight were almost stable (see also supporting information Fig. S2). This also approximately holds for the triblock copolymer $I_{15}S_{73}I_{12}^{35}$ which has a molecular weight of 35 000 g/mol and is associated with an onset of an entanglement plateau. A more complex behaviour is observed for the two triblock copolymers $S_{43}I_{20}S_{37}^{57}$ and $I_{10}S_{83}I_7^{67}$ with intermediate molecular weights. In **Fig. 5** the dynamic moduli G' and G'' as a function of time at an angular frequency of ω = 0.1 rad s^{-1} are presented.

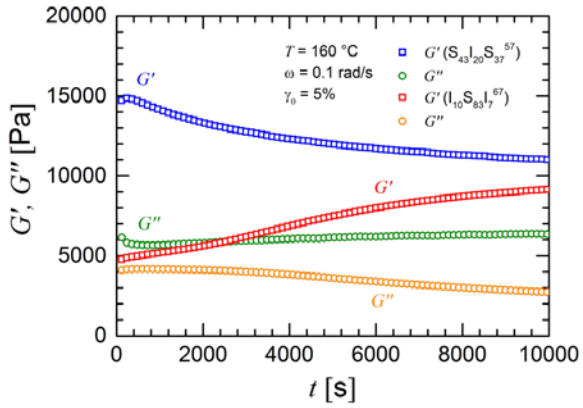

Fig. 5. Dynamic moduli G' and G'' as obtained by time sweeps at an angular frequency of ω = 0.1 rad s^{-1} for the triblock copolymers $S_{43}I_{20}S_{37}^{57}$ and $I_{10}S_{83}I_7^{67}$ at a measurement temperature of 160 °C.

The measurement temperature was 160 °C which is in both cases below the order-disorder temperature. The storage modulus G' of the triblock copolymer $S_{43}I_{20}S_{37}^{57}$ decreases with time, whereas the loss modulus G'' is approximately constant. This evolution of the dynamic moduli with time can be explained by morphological changes. A different time-dependent pattern appears for the triblock copolymer $I_{10}S_{83}I_7^{67}$ (spherical morphology) which is associated with a larger increase of storage modulus and a decrease of loss modulus with time. This behaviour reveals more "drastic"

morphological changes and is in agreement with the time evolution of the dynamic moduli of an SI diblock copolymer with a spherical morphology [67]. Our rheological data indicate that almost constant dynamic moduli are achieved for very low molecular weights (where mobility is very high and an equilibrium state is rapidly achieved) and for very high molecular weights (where mobility and dynamics are very slow and a quasi-stationary state is achieved). In the range of intermediate molecular weights mobility is significantly high and the thermodynamic driving force sufficiently strong to initiate changes of morphology and dynamic moduli.

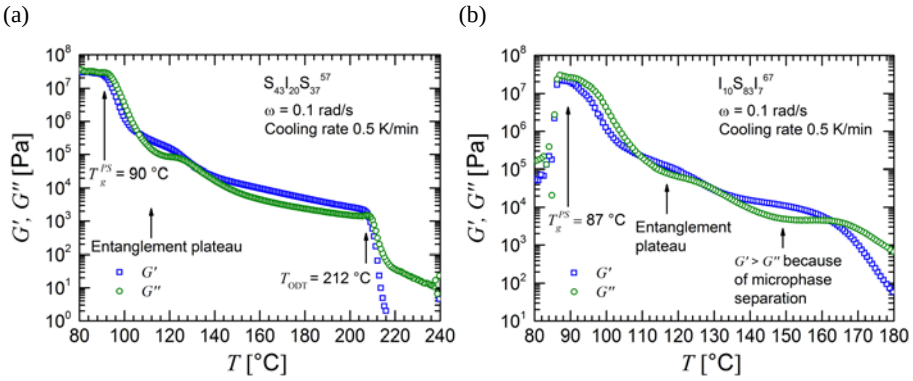

Fig. 6. Apparent dynamic moduli G' and G'' as obtained by temperature ramps at an angular frequency of ω = 0.1 rad s^{-1} and a shear amplitude γ_0 = 5% for the two triblock copolymers $S_{43}I_{20}S_{37}^{57}$ and $I_{10}S_{83}I_7^{67}$. The cooling rate was 0.5 K min^{-1}.

A qualitative picture of thermal transitions can be obtained by so-called temperature ramps which were performed at a constant angular frequency of 0.1 rad s^{-1}, a shear amplitude of 5% and a cooling rate of 0.5 K min^{-1}. We emphasize that in the temperature region around the glass transition of the major component polystyrene the stress transfer between rheometer plates and sample is imperfect leading to only apparent values of dynamic moduli. However, the temperature ramps give useful information on the overall temperature dependent viscoelastic behaviour of the triblock copolymers and are thus included in this work. Here we report on the thermal transition of the triblock copolymers with an intermediate molecular weight. In **Fig. 6**, the data are presented for the two

triblock copolymers $S_{43}I_{20}S_{37}^{57}$ and $I_{10}S_{83}I_7^{67}$. The measurements were performed from high to low temperatures. At 300 °C the triblock copolymer $S_{43}I_{20}S_{37}^{57}$ is in the disordered state with a negligible storage modulus. The dynamic moduli increase with decreasing temperature. At a temperature of 215 °C, the storage modulus strongly increases with decreasing temperature because of the order-disorder transition. Below a temperature of approximately 125 °C, the rubbery plateau is visible. At even lower temperatures the glass transition of the PS microphases can be anticipated by a maximum of the loss modulus.

A similar temperature dependence of the dynamic moduli is observed for the triblock copolymer $I_{10}S_{83}I_7^{67}$. At a temperature of 180 °C, the terminal flow regime of the disordered state is clearly visible. At a temperature of approximately 162 °C, the order-disorder transition takes place. The rubbery plateau is associated with the temperature interval from 110 to 127 °C. The maximum of the loss modulus at around 87 °C corresponds to the glass transition of the PS blocks.

The entanglement plateau above the glass transition temperature of the polystyrene blocks was analyzed based on frequency sweeps at a temperature of 120 °C, see **Fig. 7**. The plateau modulus $G_N^0 = 4\rho RT/(5M_e)$ with the density ρ, the universal gas constant R and the entanglement molecular weight M_e is associated with the minimum of the loss tangent tan δ and is listed in **Table 3**. The plateau modulus is larger for the SIS triblock copolymers than for the ISI triblock copolymers for similar total molecular weights. This effect can be explained by the isoprene blocks in the series of SIS triblock copolymers which cannot disentangle (chains tethered at both ends). Consequently, the middle isoprene block fully contributes to the storage modulus. In case of the ISI triblock copolymers, the PI blocks are not necessarily entangled and hence do not cause a pronounced contribution to the storage modulus.

Applying the method of time-temperature superposition with the software LSSHIFT [68] to the experimental data from the frequency sweep experiments at different temperatures led to master curves for the dynamic moduli (**Fig. 8**). In a strict sense, the existence of two different monomeric units with a different shift behaviour does not lead to a thermorheologically simple material. However, “apparent” master curves can be constructed and give qualitative information on the relaxation behaviour. The results presented here refer to the triblock copolymers with a low molecular weight ($S_{39}I_{22}S_{39}^{11}$, $S_{30}I_{28}S_{42}^{16}$, $I_9S_{82}I_9^{17}$), intermediate ($I_{15}S_{73}I_{12}^{35}$) and large molecular weight ($I_8S_{78}I_{14}^{98}$, $S_{35}I_{23}S_{42}^{161}$). The data superposition method was only partially possible in case of the triblock copolymers $S_{43}I_{20}S_{37}^{57}$ and $I_{10}S_{83}I_7^{67}$, since these samples undergo morphological changes

leading to significant changes of the dynamic moduli and the non-applicability of the time-temperature superposition principle due to the complexity of the material [67].

The master curves for the triblock copolymers $S_{39}I_{22}S_{39}^{11}$, $S_{30}I_{28}S_{42}^{16}$ and $I_9S_{82}I_9^{17}$ in Fig. 8(a) indicate the viscoelastic behaviour of a Maxwell fluid. The characteristic power-laws for the storage modulus $G' \sim \omega^2$ and the loss modulus $G'' \sim \omega$ (slopes 2 and 1 in a double-logarithmic presentation) are observed at low frequencies (terminal regime). In the limit of low frequencies, the zero-shear rate viscosity η_0 and the elastic equilibrium compliance J_e^0 can be calculated [60], see Table 3. Our data indicate that for a similar total molecular weight of the triblock copolymer the ISI architecture yields a higher zero shear rate viscosity than the SIS architecture. The triblock copolymer with an ISI architecture is associated with a longer styrene block as the one with an SIS architecture. In the weakly segregated regime the SIS architecture is associated with smaller coils of the polystyrene blocks than the ISI architecture. The viscosity ratio of the two triblock copolymers $I_9S_{82}I_9^{17}$ and $S_{30}I_{28}S_{42}^{16}$ is 12.4 which ranges between the limits for the viscosity ratio of unentangled polystyrene chains (Rouse model, $\eta_0 \propto M$) [69] and entangled polystyrene chains (reptation model, $\eta_0 \propto M^\nu$ with the theoretically derived result $\nu = 3$ and the experimentally determined value $\nu \approx 3.4$) [70]. Consequently, the rheological data confirm that these polymers are not fully entangled, but do not behave like Rouse chains, either.

The master curve of the $I_{15}S_{73}I_{12}^{35}$ triblock copolymer in Fig. 8(b) corresponds to an only partially entangled triblock copolymer which displays only an onset of entanglement plateau. The temperature ramp (not shown) agrees with the constructed master curve and clearly reveals the regime of glass transition and only an onset of entanglement plateau. At larger temperatures, the terminal regime can be clearly observed. This result is also supported by the SAXS measurement which does not indicate an ordered structure.

The master curves of the triblock copolymers $I_8S_{78}I_{14}^{98}$ and $S_{35}I_{23}S_{42}^{161}$ in Fig. 8(c) indicate a viscoelastic behaviour of strongly segregated block copolymers which has been also observed in a related study on diblock copolymers [67]. The transition to the glassy state of polystyrene is observed at high frequencies. The entanglement plateau is significantly larger for the SIS triblock copolymer than for the ISI triblock copolymer because of the higher molecular weight of $S_{35}I_{23}S_{42}^{161}$ and the contribution of the isoprene block being tethered to the polystyrene microphase. The cross-over of G' and G'' is observed in both cases at higher temperatures, slightly shifted to lower temperatures (higher frequencies) for the ISI triblock copolymer due to the lower molecular weight and the

different block sequence. The plateau modulus of the triblock copolymer with an ISI architecture is lower than the plateau modulus of the triblock copolymer with an SIS architecture.

The temperature dependence of the shift factor a_T of amorphous homopolymers can be generally described by the Williams-Landel-Ferry equation

$$\log(a_T) = -c_1(T - T_{\mathrm{ref}})/[c_2 + (T - T_{\mathrm{ref}})] \qquad (5)$$

with the parameters c_1 and c_2. The measurement temperature is denoted by T and the reference temperature by T_{ref} [71]. Using a least-squares fit, the material parameters c_1 and c_2 were calculated for the reference temperatures of 80, 90 and 120 °C for the different triblock copolymers according to their range of molecular weight. The WLF analysis for the two SIS triblock copolymers with the lowest molecular weights was not performed since only data for one ($S_{30}I_{28}S_{42}^{16}$) or three temperatures ($S_{39}I_{22}S_{39}^{11}$) were accessible because of the low viscosity of these samples. The results are presented in **Table 3**. The WLF fit parameters of the ISI triblock copolymers do not differ much from typical values that are observed for homopolystyrene [72]. On the contrary, the WLF parameters of the $S_{35}I_{23}S_{42}^{161}$ triblock copolymer is associated with different values of c_1 and c_2 which imply a more pronounced temperature dependence of the dynamic moduli than the ISI triblock copolymers. The Vogel temperature T_∞ is given by $T_\infty = T_{\mathrm{ref}} - c_2$ and increases with molecular weight for the ISI triblock copolymers. It is much larger for the $I_8S_{78}I_{14}^{98}$ triblock copolymer than for $S_{35}I_{23}S_{42}^{161}$. The data of the equilibrium compliance J_e^0 show similar compliance values for the block copolymers with a molecular weight in the order of 11 000 to 17 000 g/mol. The equilibrium compliance J_e^0 increases for a higher molecular weight, see the J_e^0 value for $I_{15}S_{73}I_{12}^{35}$. This result agrees with the behaviour of homopolymers for not too high molecular weights..

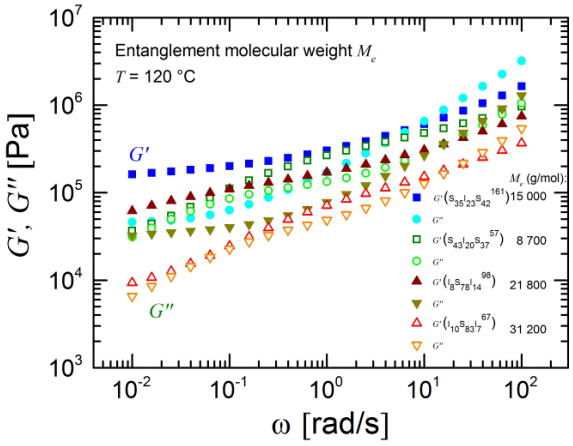

Fig. 7. Dynamic moduli G' and G'' obtained by frequency sweeps at 120 °C for four triblock copolymers depicting an entanglement plateau.

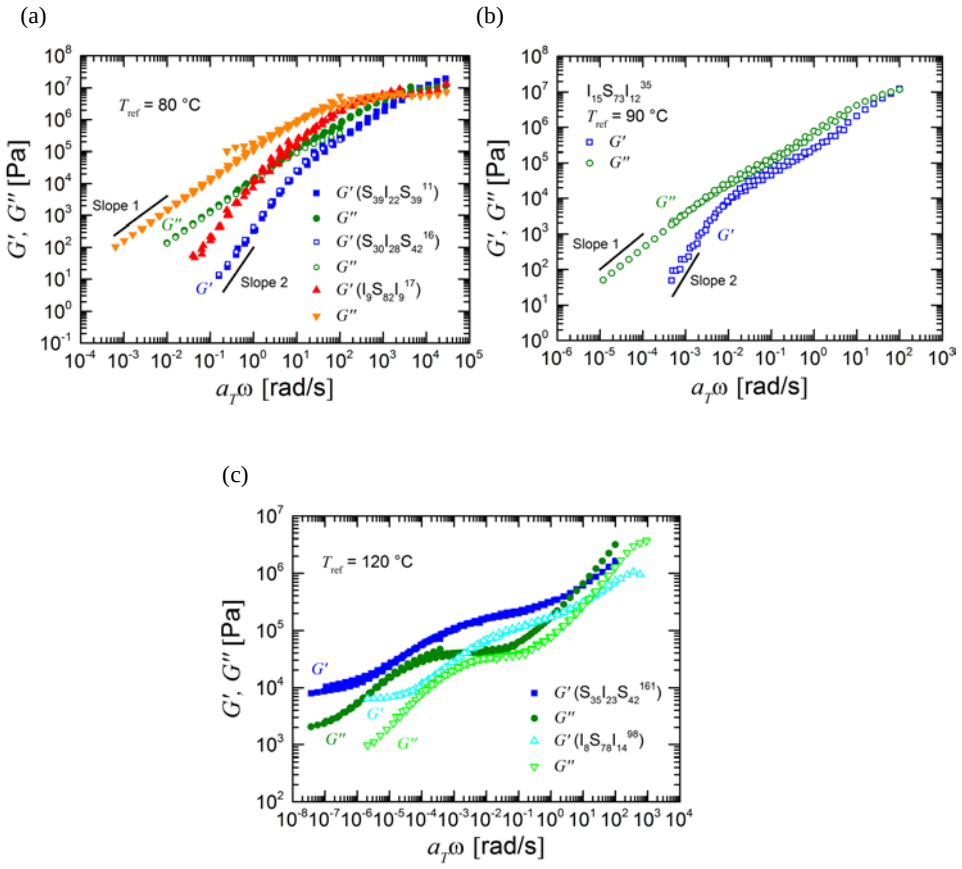

Fig. 8. Master curves created with the method of data superposition from frequency sweeps for the samples (a) $S_{39}I_{22}S_{39}^{11}$, $S_{30}I_{28}S_{42}^{16}$, $I_9S_{82}I_9^{17}$, (b) $I_{15}S_{73}I_{12}^{35}$ and (c) $I_8S_{78}I_{14}^{98}$, $S_{35}I_{23}S_{42}^{161}$ at a reference temperature of 80, 90 and 120 ºC, respectively.

Table 3. Parameters c_1 and c_2 (with standard deviation) of the WLF Eq. (5), entanglement molecular weight M_e, zero shear rate viscosity η_0 and equilibrium compliance J_e^0 for (a) SIS and (b) ISI triblock copolymers.

(a)

SIS	T_{ref} (°C)	c_1 [a]	c_2 [a] (K)	T_∞ [a] (°C)	M_e [b] (g mol^{-1})	η_0 [c] (Pa s)	J_e^0 [c] (Pa^{-1})
$S_{39}I_{22}S_{39}$[11]	80	-	-	-	-	13 900	2.6 x 10^{-6}
$S_{30}I_{28}S_{42}$[16]	80	-	-	-	-	13 300	2.7 x 10^{-6}
$S_{43}I_{20}S_{37}$[57]	120	-	-	-	8 700	-	-
$S_{35}I_{23}S_{42}$[161]	120	10.4±0.4	90.2±5.8	29.8	15 000	-	-

(b)

ISI	T_{ref} (°C)	c_1 [a]	c_2 [a] (K)	T_∞ [a] (°C)	M_e [b] (g mol^{-1})	η_0 [c] (Pa s)	J_e^0 [c] (Pa^{-1})
$I_9S_{82}I_9$[17]	80	4.8±1.7	58.1±14.8	21.9	-	165 000	1.3 x 10^{-6}
$I_{15}S_{73}I_{12}$[35]	90	7.9±0.1	51.0±0.8	39.0	-	4 150 000	1.3 x 10^{-5}
$I_{10}S_{83}I_7$[67]	120	-	-	-	31 200	-	-
$I_8S_{78}I_{14}$[98]	120	6.8±0.4	53.4±5.5	66.6	21 800	-	-

[a] Determined from the fit of the WLF equation and $T_\infty = T_{ref} - c_2$. [b] Calculated using $M_e = 4\rho RT/(5G_N^0)$. [c] Calculated at reference temperature T_{ref} from the power-law regime in case of Maxwell fluid behaviour at low frequencies

3.6 Broadband dielectric spectroscopy

In styrene - *cis*-1,4-isoprene block copolymers generally three dipole moments contribute to the complex dielectric permittivity $\varepsilon^* = \varepsilon' - i\varepsilon''$, i.e. the perpendicular component of the dipole moment of the polyisoprene block (sensitive to segmental relaxation), the parallel component of the dipole moment of the PI block (sensitive to normal mode relaxation) and the dipole moment of the polystyrene block (sensitive to segmental relaxation). Since the dielectric strength $\Delta\varepsilon_n$ of the normal mode is given by [73]

$$\Delta\varepsilon_n = \frac{N_A \mu^2 \langle r^2 \rangle \Phi^{PI}}{3 k_B T M^{PI}} \quad (6)$$

where Φ^{PI} denotes the volume fraction of the PI block, μ the dipole moment per contour length, N_A the Avogadro constant, k_B the Boltzmann constant, $\langle r^2 \rangle$ the mean square distance of the end-to-end

vector and M^{PI} the molecular weight of the polyisoprene block, the magnitude of the complex permittivity caused by the normal mode relaxation decreases with molecular weight. Therefore the normal mode relaxation should be more clearly detected for a low molecular weight block copolymer. However, miscibility of the PS and the PI microphases increases with a decreasing molecular weight. Furthermore, since in our case the weight fraction f^{PI} of the polyisoprene block does not exceed 28%, the dielectric strength of the normal mode relaxation only is moderately pronounced or almost suppressed [2]. Dielectric spectroscopic data on SI diblock copolymers [73] also indicate that the segmental relaxation of the PI block can only be hardly seen for very low PI fractions or even not at all [74]. For low PI fractions, the dynamics of microphase separation can be terminated by the glass transition of the PS block such that no PI microdomain is developed and the normal mode of the PI block is not observed [74].

Temperature ramp experiments give a qualitative overview on the temperature-dependent dielectric response, i.e. in particular on the intensity of the normal mode relaxation. In **Fig. 9** the results of the temperature ramps of non-annealed samples at a frequency of 10 Hz for the SIS and ISI triblock copolymers are presented. The dielectric loss ε'' is plotted as a function of temperature in order to monitor the relaxation processes of the triblock copolymers. Similar to the discussion of the rheological data, the triblock copolymers are grouped based on their total molecular weight into low molecular weight ($S_{39}I_{22}S_{39}^{11}$, $S_{30}I_{28}S_{42}^{16}$, $I_9S_{82}I_9^{17}$), intermediate ($I_{15}S_{73}I_{12}^{35}$, $S_{43}I_{20}S_{37}^{57}$, $I_{10}S_{83}I_7^{67}$) and large molecular weight ($I_8S_{78}I_{14}^{98}$, $S_{35}I_{23}S_{42}^{161}$) triblock copolymers.

For the low molecular weight triblock copolymers (Fig. 9(a)) the dynamic glass transition temperature of the PS and the PI microphases strongly depends on the miscibility of the two blocks. The triblock copolymer $S_{39}I_{22}S_{39}^{11}$ is associated with four relaxation processes with peaks at approximately -20 °C (PI segmental mode), 60 °C (PS segmental mode) and a third process at 90 °C. A fourth relaxation process at very high temperatures can be also detected. The curve of the triblock copolymer $S_{30}I_{28}S_{42}^{16}$ shows three processes, the segmental PI mode at -40 °C, the PS segmental mode at 60 °C and a third process at 90 °C. The normal mode relaxation caused by the PI middle block in the SIS triblock copolymers is strongly suppressed since the PI block is confined to an interfacial region between the PS and the PI microphases, see also Alig et al. [50]. In the case of the triblock copolymer $S_{30}I_{28}S_{42}^{16}$ the interfacial region is broad because of the partial miscibility of the PS and the PI blocks. The miscibility of the PI blocks of the triblock copolymer $I_9S_{82}I_9^{17}$ with the PS blocks is more pronounced than for the triblock copolymer $S_{30}I_{28}S_{42}^{16}$ since the PI blocks of the ISI

copolymer are shorter than the PI block of the SIS copolymer. The triblock copolymer $I_9S_{82}I_9^{17}$ shows three relaxation processes which correspond to the PI segmental relaxation (weakly pronounced), the PI normal mode and the PS segmental relaxation in the mixed PS/PI domain. In contrast to the DSC experiments, dielectric spectroscopy allows for detecting the PI segmental relaxation even for low PI fractions because of its dipole moment.

Increasing the molecular weight yields a less pronounced peak of normal mode relaxation (cf. Eq. (6)) and a larger degree of microphase separation. In case of the intermediate molecular weight triblock copolymers $I_{15}S_{73}I_{12}^{35}$, $S_{43}I_{20}S_{37}^{57}$ and $I_{10}S_{83}I_7^{67}$ the dynamic glass transition of the polyisoprene and the polystyrene block are observed at -60 °C to -40 °C and 70 °C to 120 °C, respectively. The effect of dc conductivity appears at temperatures above 120 °C. The normal mode relaxation of the ISI triblock copolymers is mainly seen for the triblock copolymer $I_{10}S_{83}I_7^{67}$ (because of a larger degree of microphase separation) and observed in the temperature interval from -40 °C to 0 °C. Since in case of the SIS triblock copolymer the polyisoprene block is fixed between the two glassy polystyrene blocks, decreasing the mobility of the PI chains to a finite value, the SIS triblock copolymer is associated with a less pronounced normal mode relaxation at a slightly higher temperature range (-20 °C to 40 °C) [50].

The data for the two triblock copolymers with a high molecular weight ($I_8S_{78}I_{14}^{98}$, $S_{35}I_{23}S_{42}^{161}$) show the segmental relaxation of the PI and the PS blocks (Fig. 9(c)). The temperature difference of the peak maxima of the segmental relaxation attains the highest value for these two triblock copolymers, since a larger molecular weight yields a larger degree of microphase separation. Generally, the peak intensity of normal mode relaxation of PI blocks decreases with increasing molecular weight (Eq. (6)). Therefore the normal mode relaxation of the triblock copolymer $I_8S_{78}I_{14}^{98}$ only is associated with a low peak height. In summary, the temperature ramp experiments indicate that the SIS block sequence yields a strong suppression of the normal mode.

Isothermal frequency sweeps were carried out in order to get a more quantitative view on the relaxation processes. **Fig. 10** presents the dielectric loss ε'' as a function of frequency at constant temperature for selected triblock copolymers. The triblock copolymer $I_9S_{82}I_9^{17}$ is an example for a low molecular weight triblock copolymer. **Fig. 10(a)** presents the frequency dependent dielectric loss ε'' in the temperature interval around the glass transition of the mixed PS/PI domain. The data for the triblock copolymer $S_{39}I_{20}S_{39}^{11}$ clearly show the presence of several relaxation processes (PS and PI segmental relaxation and a third process at very low frequencies), see Fig. 10(b). In the case of an

intermediate molecular weight, the data of the triblock copolymer $I_{15}S_{73}I_{12}^{35}$ are presented in **Fig. 10(c)**. A very broad relaxation process is observed which possibly can be contributed to the segmental and normal modes of the PI blocks. This relaxation process of the triblock copolymer $I_{15}S_{73}I_{12}^{35}$ seems to be affected by the polystyrene block (being partially miscible with the PI block) which leads to the broadening of the process. The broadening of the normal mode was theoretically [75] and experimentally [73, 76] studied. The data in **Fig. 10(d)** for the triblock copolymer $S_{35}I_{23}S_{42}^{161}$ indicate the glass transition of the PI block. They also reveal that normal mode relaxation is suppressed.

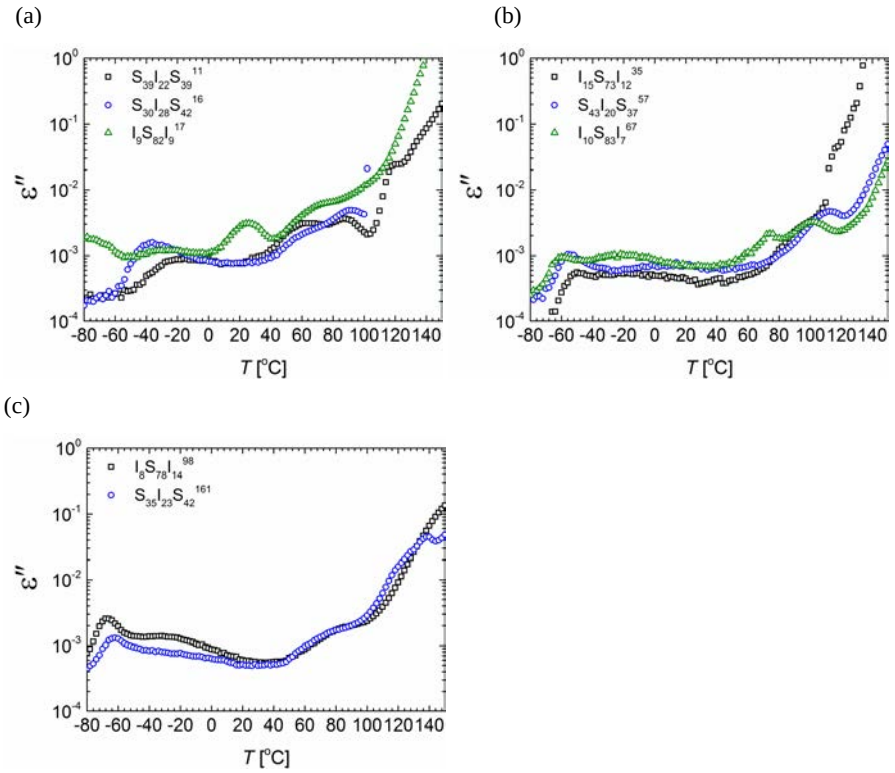

Fig. 9. Temperature ramp experiments for the (a) $S_{39}I_{22}S_{39}^{11}$, $S_{30}I_{28}S_{42}^{16}$ and $I_9S_{82}I_9^{17}$, (b) $I_{15}S_{73}I_{12}^{35}$, $S_{43}I_{20}S_{37}^{57}$ and $I_{10}S_{83}I_7^{67}$ (c) $I_8S_{78}I_{14}^{98}$ and $S_{35}I_{23}S_{42}^{161}$ triblock copolymer. The dielectric loss ε'' is plotted as a function of temperature. The frequency was 10 Hz.

The Havriliak-Negami [77] (HN) function including a conductivity contribution is usually applied to describe experimental data ($\omega=2\pi f$):

$$\varepsilon^* = \varepsilon' - i\varepsilon'' = -i\left(\frac{\sigma_0}{\epsilon_0\omega}\right)^s + \varepsilon_\infty + \frac{\Delta\varepsilon}{(1+(i\omega\tau)^\alpha)^\beta} \quad (7)$$

In Eq. (7) σ_0 denotes the dc conductivity, the parameter s an exponent which attains $s = 1$ for purely ohmic conductivity and $s < 1$ for non-ohmic conductivity, ε_0 the permittivity of the vacuum and $\Delta\varepsilon$ the dielectric strength. The parameters α,β are additional fit parameters which describe the shape of the curve (α the broadness and β the asymmetry of the curve). The parameter ε_∞ is the high frequency limit of the dielectric permittivity. The relaxation time is denoted by τ. In this work, the imaginary part of Eq. (7) was fitted to the experimental data. The parameter σ_0 was set to zero for fits in the temperature range near the glass transition temperature of the PI block (Table 4(a)). **Figure 11** presents the fitted Eq. (7) at selected temperatures (cf. **Table 4**). The data in Table 4(a) describe the segmental relaxation of the PI block. The value of the shape parameter α for the SIS triblock copolymers is in the order of 0.5 which is typical for the α-process[78]. The data reveal the effect of molecular weight on miscibility of the PS and the PI blocks and thus on the position (i.e. the inverse relaxation time) of the relaxation peaks. A larger molecular weight yields a more pronounced phase separation and a larger difference of the temperature of the dynamical glass transition of the PS and the PI blocks.

Because of suppression of the normal mode for SIS triblock copolymers, only the segmental mode of the PI block and of the PS block of the SIS triblock copolymers are analyzed. **Fig. 12**(a) shows the influence of the molecular weight on the segmental-mode for the SIS triblock copolymers and presents the frequency f_{max} at peak maximum as a function of inverse temperature $1/T$. The relaxation process is strongly influenced by the miscibility of the PI and the PS blocks and consequently by the total molecular weight. Generally, the relaxation rates decrease with decreasing temperature. A WLF fit to the maximum frequency f_{max} as a function of temperature T using the equation

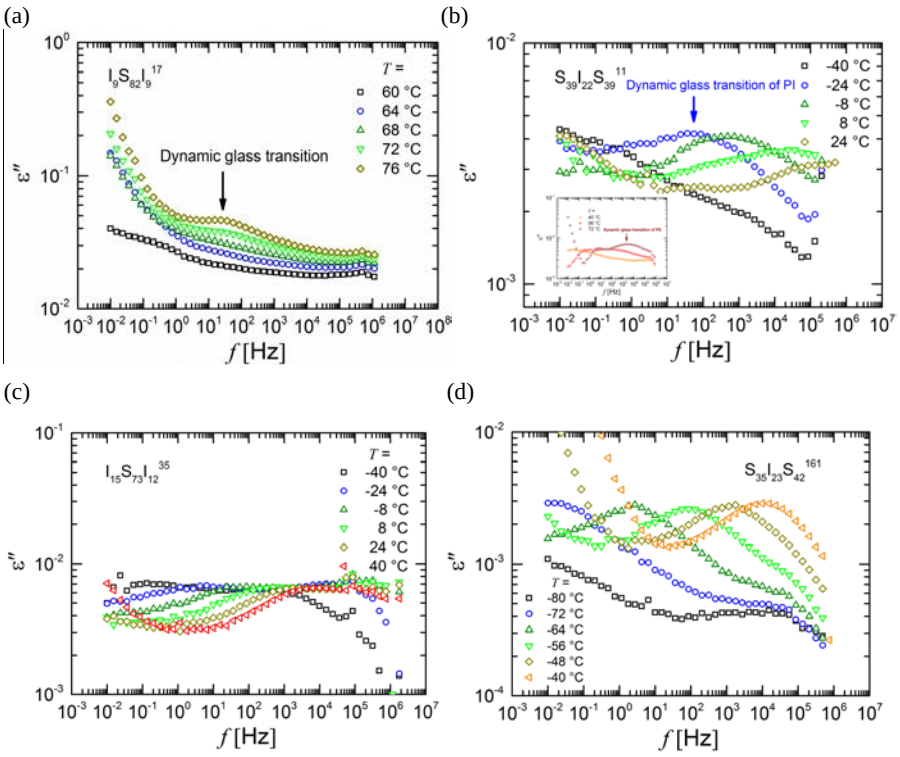

Fig. 10. Dielectric loss ε'' as a function of frequency for the triblock copolymers (a) $I_9S_{82}I_9^{17}$, (b) $S_{39}I_{22}S_{39}^{11}$, (c) $I_{15}S_{73}I_{12}^{35}$ and (d) $S_{35}I_{23}S_{42}^{161}$ at various temperatures.

$$\log(f_{\max}) = \log(f_\infty) + \frac{c_1(T-T_{\text{ref}})}{c_2+T-T_{\text{ref}}} \quad (8)$$

with the reference temperature T_{ref}, the frequency f_∞ at peak maximum at reference temperature and the parameters c_1 and c_2 was performed. The result of the fit is indicated by the solid lines in Fig. 12 (see **Table 5**). The Vogel temperature $T_\infty = T_{\text{ref}} - c_2$ based on the segmental mode relaxation of the PI and the PS blocks, respectively, is also listed. The Vogel temperature generally increases with molecular weight and thus follows the typical behaviour of polymers. The curves for the segmental mode of polyisoprene are shifted to lower temperatures with increasing molecular weight because of

a decreasing miscibility. Comparing the results of the PI segmental relaxation with the results on PI homopolymers in the work of Boese and Kremer [79] the relaxation rates in case of the triblock copolymers appear thus to be affected by the miscibility of the PS block with the PI block.

Fig. 12(b) presents the activation plot for the segmental mode of polystyrene of the SIS triblock copolymers. The relative relaxation rate strongly depends on the molecular weight and the miscibility of the two blocks. A lower molecular weight yields a shift of the curve to higher inverse temperatures.

The segmental relaxation of the ISI triblock copolymers are strongly influenced by the molecular weight. **Fig. 12**(c) presents the peak frequency of the segmental mode of the PI block as a function of inverse temperature. The segmental mode of the PI block of the ISI triblock copolymers might be also superposed by the β relaxation of the polystyrene block. A low molecular weight implies a partial miscibility of the PS and the PI blocks leading to a strong influence of the PS block on the dynamics of the PI block and to a shift of the curve with higher molecular weight to lower temperatures. In Fig. 12(d) the activation plot for the segmental mode of polystyrene is shown. Similar to the SIS triblock copolymers, a larger molecular weight yields a shift of the curve to lower inverse temperatures.

Generally, the normal mode of the ISI triblock copolymers was relatively broad which was a general feature of the experimental data and complicated their analysis. Therefore normal mode relaxation could only be analyzed for the $I_{15}S_{73}I_{12}^{35}$ and $I_8S_{78}I_{14}^{98}$ triblock copolymers which are associated with a higher weight fraction of polyisoprene. The corresponding activation plot is shown in Fig. 12(e). In spite of the different molecular weights of the triblock copolymers, similar relative relaxation rates for both triblock copolymers are observed. This is also revealed by the WLF parameters in Table 5(b) (normal mode relaxation) which show a different behaviour than the values in Table 5(a) (segmental mode relaxation).

(a) (b)

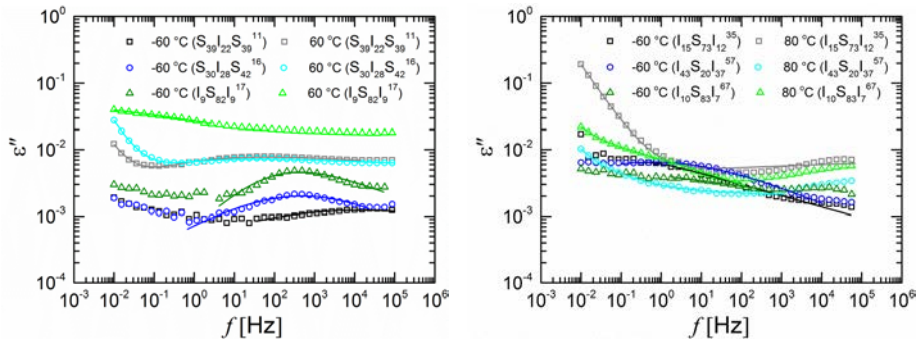

(c)

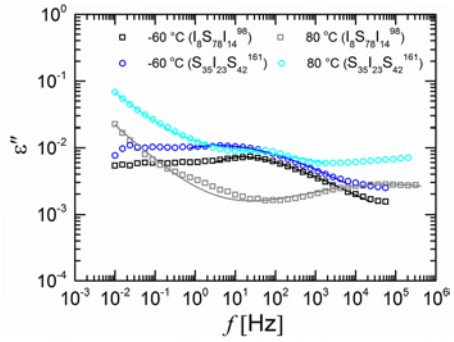

Fig. 11. Results of the applied fits of the HN function Eq. (7) to the experimental ε'' data for the triblock copolymers of this study: (a) $S_{39}I_{22}S_{39}^{11}$, $S_{30}I_{28}S_{42}^{16}$ and $I_9S_{82}I_9^{17}$, (b) $I_{15}S_{73}I_{12}^{35}$, $S_{43}I_{20}S_{37}^{57}$ and $I_{10}S_{83}I_7^{67}$ (c) $I_8S_{78}I_{14}^{98}$ and $S_{35}I_{23}S_{42}^{161}$ triblock copolymer.

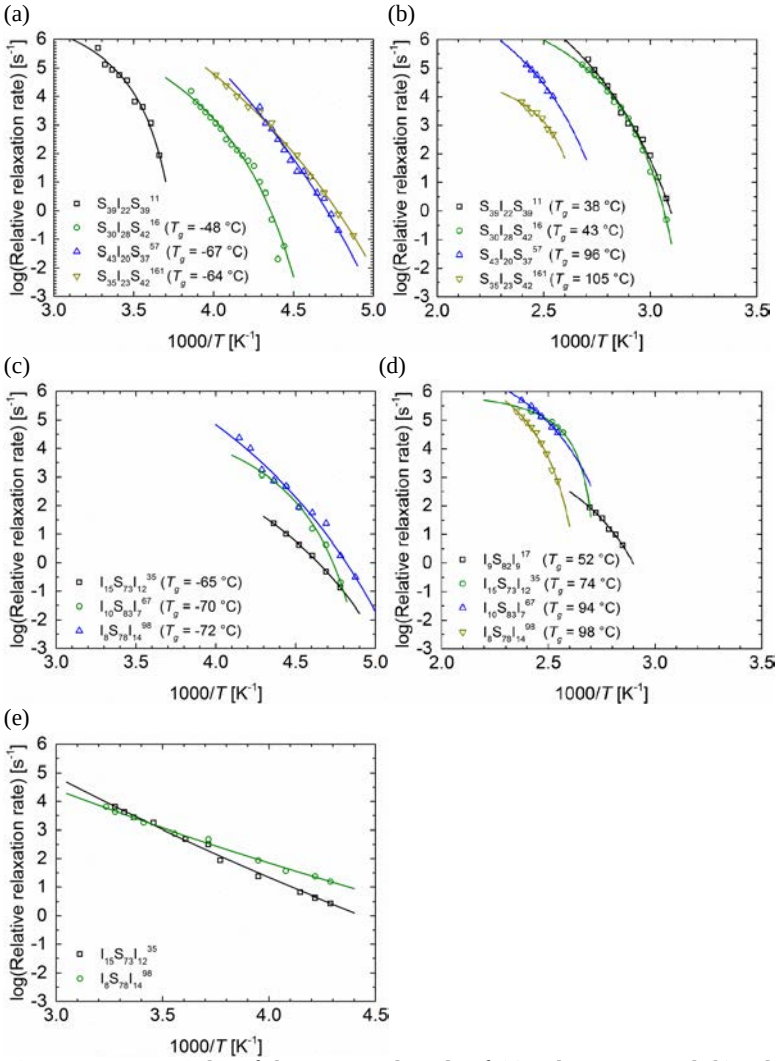

Fig. 12. Activation plot of the segmental mode of (a) polyisoprene and (b) polystyrene for the SIS triblock copolymers of this study. Activation plot of the segmental mode of (c) polyisoprene and (d) polystyrene for the ISI triblock copolymers $I_9S_{82}I_9^{17}$ (only polystyrene segmental mode), $I_{15}S_{73}I_{12}^{35}$, $I_{10}S_{83}I_7^{67}$ and $I_8S_{78}I_{14}^{98}$. (e) Activation plot of the normal mode of polyisoprene for the triblock copolymers $I_{15}S_{73}I_{12}^{35}$ and $I_8S_{78}I_{14}^{98}$. A fit of the WLF Eq. (8) is indicated by solid lines.

Table 4. Fit parameters of the HN function Eq. (7) including a conductivity term at a low (-60 °C) and a higher temperature (60 °C and 80 °C, respectively) for each triblock copolymer. In (a) the conductivity parameter σ_0 was set to zero. In (b) for the $I_8S_{78}I_{14}^{98}$ triblock copolymer two HN modes were used for fitting the data (denoted by HN1 and HN2).

(a)

Samples	T (°C)	$\Delta\varepsilon$ (10^{-2})	τ (s)	α	β	Mean squared deviation of HN Fit
SIS						
$S_{39}I_{22}S_{39}^{11}$	-60	1.49	1.13×10^{-5}	0.21	1.00	0.48×10^{-4}
$S_{30}I_{28}S_{42}^{16}$	-60	1.44	3.24×10^{-4}	0.35	1.00	0.90×10^{-4}
$S_{43}I_{20}S_{37}^{57}$	-60	5.89	3.11×10^{-1}	0.28	0.94	1.24×10^{-4}
$S_{35}I_{23}S_{42}^{161}$	-60	7.93	4.65×10^{-2}	0.34	0.96	1.50×10^{-4}
ISI						
$I_9S_{82}I_9^{17}$	-60	2.90	1.66×10^{-3}	0.55	0.42	2.57×10^{-4}
$I_{15}S_{73}I_{12}^{35}$	-60	3.71	1.69×10^{0}	1.00	0.17	1.92×10^{-4}
$I_{10}S_{83}I_7^{67}$	-60	5.73	1.36×10^{0}	0.18	1.00	0.61×10^{-4}
$I_8S_{78}I_{14}^{98}$	-60	3.98	3.12×10^{-2}	0.58	0.50	0.84×10^{-4}

(b)

Samples	T (°C)	σ_0 (10^{-17} S/cm)	s	$\Delta\varepsilon$ (10^{-2})	τ (s)	α	β	Mean squared deviation of HN fit
SIS								
$S_{39}I_{22}S_{39}^{11}$	60	5.29	1.0	19.70	1.13×10^{0}	0.41	0.08	1.26×10^{-4}
$S_{30}I_{28}S_{42}^{16}$	60	13.74	1.0	232.00	2.25×10^{0}	0.45	0.05	1.88×10^{-4}
$S_{43}I_{20}S_{37}^{57}$	80	0.18	0.6	15.10	3.88×10^{0}	0.01	0.01	0.86×10^{-4}
$S_{35}I_{23}S_{42}^{161}$	80	2.72	0.5	8.20	0.01×10^{0}	0.24	1.00	0.54×10^{-4}
ISI								
$I_9S_{82}I_9^{17}$	60	-	-	79.20	3.85×10^{4}	0.17	0.73	4.99×10^{-4}
$I_{15}S_{73}I_{12}^{35}$	80	8.56	0.9	31.30	1.13×10^{-11}	0.57	1.00	1.21×10^{0}
$I_{10}S_{83}I_7^{67}$	80	4.67	1.0	16.00	1.15×10^{3}	0.27	0.76	2.14×10^{-4}
$I_8S_{78}I_{14}^{98}$ HN1	80	51.67	0.6	9.50	1.00×10^{5}	1.00	0.01	4.30×10^{-4}
$I_8S_{78}I_{14}^{98}$ HN2	80	-	-	1.70	8.23×10^{-6}	0.34	0.68	4.30×10^{-4}

Table 5. Parameters c_1 and c_2 of the WLF Eq. (8) (with standard deviation) for the (a) PI segmental mode relaxation, (b) PI normal mode relaxation and (c) PS segmental mode relaxation. The Vogel temperature $T_\infty = T_{\text{ref}} - c_2$ is also listed.

(a)

SIS	T_{ref} (°C)	c_1	c_2 (K)	T_∞ (°C)	f_∞ (Hz)
$S_{39}I_{22}S_{39}^{11}$	0	5.9±0.7	21.2±4.9	-21	86.5
$S_{30}I_{28}S_{42}^{16}$	-48	9.8±0.3	30.1±1.2	-78	0.1
$S_{43}I_{20}S_{37}^{57}$	-64	16.4±5.6	72.8±30.9	-137	0.2
$S_{35}I_{23}S_{42}^{161}$	-68	13.7±1.0	63.9±6.7	-132	0.1
ISI	T_{ref} (°C)	c_1	c_2 (K)	T_∞ (°C)	f_∞ (Hz)
$I_9S_{82}I_9^{17}$	-	-	-	-	-
$I_{15}S_{73}I_{12}^{35}$	-64	7.7±0.9	48.7±7.2	-113	0.1
$I_{10}S_{83}I_7^{67}$	-64	6.8±0.8	18.6±4.0	-83	0.2
$I_8S_{78}I_{14}^{98}$	-68	12.1±2.6	56.5±18.0	-125	0.3

(b)

ISI	T_{ref} (°C)	c_1	c_2 (K)	f_∞ (Hz)
$I_{15}S_{73}I_{12}^{35}$	-40	21.4±9.9	383.5±204.4	2.7
$I_8S_{78}I_{14}^{98}$	-40	15.1±6.3	369.2±180.4	15.4

(c)

SIS	T_{ref} (°C)	c_1	c_2 (K)	T_∞ (°C)	f_∞ (Hz)
$S_{39}I_{22}S_{39}^{11}$	52	11.0±1.1	57.8±9.2	-6	2.7
$S_{30}I_{28}S_{42}^{16}$	52	8.8±0.5	30.1±3.5	22	0.5
$S_{43}I_{20}S_{37}^{57}$	120	5.8±3.5	83.0±60.5	37	1.0×10^4
$S_{35}I_{23}S_{42}^{161}$	120	2.7±1.0	36.1±19.3	84	4.9×10^2
ISI	T_{ref} (°C)	c_1	c_2 (K)	T_∞ (°C)	f_∞ (Hz)
$I_9S_{82}I_9^{17}$	78	4.8±1.6	53.1±22.8	25	4.2
$I_{15}S_{73}I_{12}^{35}$	116	1.7±0.2	29.3±5.7	87	3.7×10^4
$I_{10}S_{83}I_7^{67}$	120	4.2±1.1	74.0±25.7	46	3.7×10^4
$I_8S_{78}I_{14}^{98}$	120	5.3±0.5	36.7±6.0	83	7.5×10^2

4. Conclusions

Our analysis of the influence of block sequence and molecular weight of styrene-isoprene triblock copolymers with polystyrene as the majority component on the thermal, viscoelastic and dielectric properties clearly reveal the dominating effect of molecular weight of the styrene and isoprene blocks and the block sequence on the relaxation behaviour of triblock copolymers. In case of a low molecular weight, the glass transition temperature of the polystyrene block is shifted to lower values, indicating weak microphase segregation. Applying the Fox-Flory model the penetration of one block into the other was estimated. The combination of the Fox-Flory and the Bicerano equations underestimates the influence of polyisoprene and yield larger polyisoprene fractions than the real composition. The increase of the molecular weight causes the decrease of penetration of each block into the corresponding second block. The higher molecular weight triblock copolymers clearly exhibit the glass transition temperatures similar to the values of the corresponding homopolymers, indicating pronounced microphase separation which was also verified by SAXS and TEM investigations. Three of the triblock copolymers in the strong segregation limit were associated with a cylindrical structure. In case of the $I_{10}S_{83}I_7^{67}$ triblock copolymer the SAXS analysis and TEM investigations indicated a spherical morphology. Rheological experiments in the melt state show the Maxwell fluid behaviour (corresponding to the disordered state) in case of the samples with a molecular weight below the entanglement molecular weight. Indication of the microphase separation of the two components was observed for the block copolymers with higher molecular weights (plateau of storage modulus at low frequencies). The dynamic moduli were associated with an entanglement plateau if the molecular weight was above the entanglement molecular weight. An important aspect was the influence of the block sequence on the plateau modulus G_N^o and the zero shear rate viscosity η_0 for the Maxwell fluids. The middle PI block of SIS triblock copolymers significantly contributes to the plateau modulus leading to larger G_N^o value for the SIS triblock copolymers than for the ISI triblock copolymers. The zero shear rate viscosity of the SIS triblock copolymers with a low molecular weight generally was much smaller than the zero shear rate viscosity of the ISI triblock copolymers with a comparable total molecular weight because of the shorter PS blocks at the ends of the triblock polymer chain (lower molecular weight of the single PS blocks). The dielectric spectroscopy data are strongly influenced by the molecular weight of the triblock copolymer which determines the miscibility of the PS and the PI blocks and the dielectric

strength of the normal mode. The normal mode relaxation corresponding to the 1,4-polyisoprene block was hindered to a large extent for the SIS triblock copolymers in comparison with the ISI triblock copolymers, due to the fact that the PI blocks are tethered between the glassy PS blocks. Furthermore the normal mode relaxation of the PI block of the ISI triblock copolymers can be preferentially observed for molecular weights which imply a compromise of sufficient segregation and dielectric strength. In summary, our experimental data reveal that the block sequence in triblock copolymers influences dynamical properties of these polymers.

Acknowledgement

The authors thank Mr. Silvio Neumann for DSC and NMR experiments, Mrs. Maren Brinkmann for GPC measurements and Mrs. Ivonne Ternes for rheological experiments, Dr. Vasyl Haramus for his assistance with SAXS experiments and Dr. Thomas Emmler for experimental support. The valuable discussions with Dr. Dirk Wilmer (Novocontrol Technologies GmbH) and comments by Prof. Friedrich Kremer are also gratefully acknowledged. This work received financial support from the German Research Foundation (DFG) via SFB 986 "M^3", project A2.

Graphical Abstract

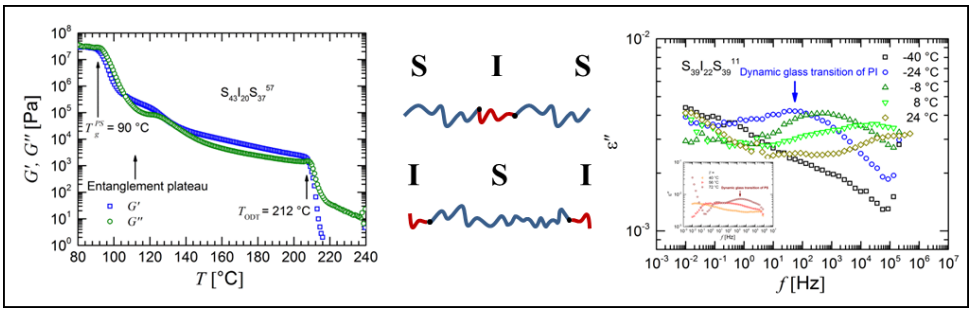

References

1. Bates FS and Fredrickson GH. Physics Today 1999;52(2):32.
2. Hadjichristidis N, Pispas S, and Floudas G. Block copolymers: synthetic strategies, physical properties, and applications: John Wiley & Sons, 2003.
3. Bates FS, Hillmyer MA, Lodge TP, Bates CM, Delaney KT, and Fredrickson GH. Science 2012;336(6080):434-440.
4. Boschetti-de-Fierro A and Abetz V. 7.02 - Block Copolymer in the Condensed State. Polymer Science: A Comprehensive Reference, vol. 7. Amsterdam: Elsevier, 2012. pp. 3-44.
5. Auschra C, Stadler R, and Voigt-Martin IG. Polymer 1993;34(10):2081-2093.
6. Auschra C, Stadler R, and Voigt-Martin IG. Polymer 1993;34(10):2094-2110.
7. Auschra C and Stadler R. Macromolecules 1993;26(9):2171-2174.
8. Kirschnick T, Gottschalk A, Ott H, Abetz V, Puskas J, and Altstädt V. Polymer 2004;45(16):5653-5660.
9. Ruckdäschel H, Sandler JK, Altstädt V, Rettig C, Schmalz H, Abetz V, and Müller AH. Polymer 2006;47(8):2772-2790.
10. Bahrami R, Löbling TI, Schmalz H, Müller AH, and Altstädt V. Polymer 2015;80:52-63.
11. Goldacker T, Abetz V, Stadler R, Erukhimovich I, and Leibler L. Nature 1999;398(6723):137-139.
12. Abetz V and Goldacker T. Macromolecular Rapid Communications 2000;21(1):16-34.
13. Chao C-C, Wang T-C, Ho R-M, Georgopanos P, Avgeropoulos A, and Thomas EL. ACS Nano 2010;4(4):2088-2094.
14. Darling S. Progress in Polymer Science 2007;32(10):1152-1204.
15. Carrasco P, Tzounis L, Mompean F, Strati K, Georgopanos P, Garcia-Hernandez M, Stamm M, Cabanero G, Odriozola I, and Avgeropoulos A. Macromolecules 2013;46(5):1860-1867.
16. Park C, Yoon J, and Thomas EL. Polymer 2003;44(22):6725-6760.
17. Hoon Kim B, Young Kim J, and Ouk Kim S. Soft Matter 2013;9(10):2780-2786.
18. Shin DO, Mun JH, Hwang G-T, Yoon JM, Kim JY, Yun JM, Yang Y-B, Oh Y, Lee JY, and Shin J. ACS Nano 2013;7(10):8899-8907.
19. Abetz V. Macromolecular Rapid Communications 2015;36(1):10-22.
20. Radjabian M, Koll J, Buhr K, Vainio U, Abetz C, Handge UA, and Abetz V. Polymer 2014;55(13):2986-2997.
21. Radjabian M and Abetz V. Advanced Materials 2015;27(2):352-355.
22. Clodt JI, Filiz V, Rangou S, Buhr K, Abetz C, Höche D, Hahn J, Jung A, and Abetz V. Advanced Functional Materials 2013;23(6):731-738.
23. Phillip WA, Hillmyer MA, and Cussler E. Macromolecules 2010;43(18):7763-7770.
24. Phillip WA, Mika Dorin R, Werner Jr, Hoek EM, Wiesner U, and Elimelech M. Nano Letters 2011;11(7):2892-2900.
25. Mulvenna RA, Weidman JL, Jing B, Pople JA, Zhu Y, Boudouris BW, and Phillip WA. Journal of Membrane Science 2014;470:246-256.
26. Rahman MM, Filiz V, Shishatskiy S, Abetz C, Georgopanos P, Khan MM, Neumann S, and Abetz V. ACS Applied Materials & Interfaces 2014.
27. Rahman MM, Shishatskiy S, Abetz C, Georgopanos P, Neumann S, Khan MM, Filiz V, and Abetz V. Journal of Membrane Science 2014;469:344-354.
28. Stadler R, Auschra C, Beckmann J, Krappe U, Voight-Martin I, and Leibler L. Macromolecules 1995;28(9):3080-3097.
29. Breiner U, Krappe U, Abetz V, and Stadler R. Macromolecular Chemistry and Physics 1997;198(4):1051-1083.
30. Hückstädt H, Göpfert A, and Abetz V. Polymer 2000;41(26):9089-9094.
31. Ludwigs S, Böker A, Abetz V, Müller AH, and Krausch G. Polymer 2003;44(22):6815-6823.
32. Schmalz H, Knoll A, Müller AJ, and Abetz V. Macromolecules 2002;35(27):10004-10013.
33. Balsamo V, Gil G, Urbina de Navarro C, Hamley I, Von Gyldenfeldt F, Abetz V, and Canizales E. Macromolecules 2003;36(12):4515-4525.
34. Ott H, Abetz V, and Altstädt V. Macromolecules 2001;34(7):2121-2128.
35. Breiner U, Krappe U, Thomas EL, and Stadler R. Macromolecules 1998;31(1):135-141.
36. Epps TH, Cochran EW, Hardy CM, Bailey TS, Waletzko RS, and Bates FS. Macromolecules 2004;37(19):7085-7088.

37. Schmalz H, Böker A, Lange R, Krausch G, and Abetz V. Macromolecules 2001;34(25):8720-8729.
38. Matsen M and Bates F. Macromolecules 1996;29(4):1091-1098.
39. Gehlsen MD, Almdal K, and Bates FS. Macromolecules 1992;25(2):939-943.
40. Riess G. Progress in Polymer Science 2003;28(7):1107-1170.
41. Matsen MW and Schick M. Macromolecules 1994;27(1):187-192.
42. Laurer J, Khan S, Spontak R, Satkowski M, Grothaus J, Smith S, and Lin J. Langmuir 1999;15(23):7947-7955.
43. Laurer JH, Hajduk DA, Fung JC, Sedat JW, Smith SD, Gruner SM, Agard DA, and Spontak RJ. Macromolecules 1997;30(13):3938-3941.
44. Matsuo Y, Konno R, Ishizone T, Goseki R, and Hirao A. Polymers 2013;5(3):1012-1040.
45. Davis KA and Matyjaszewski K. Macromolecules 2001;34(7):2101-2107.
46. Agudelo NA, Elsen AM, He H, López BL, and Matyjaszewski K. Journal of Polymer Science Part A: Polymer Chemistry 2015;53(2):228-238.
47. Brandt H-D, Nentwig W, Rooney N, LaFlair RT, Wolf UU, Duffy J, Puskas JE, Kaszas G, Drewitt M, and Glander S. Rubber, 5. Solution Rubbers. Ullmann's Encyclopedia of Industrial Chemistry: Wiley-VCH Verlag GmbH & Co. KGaA, 2000.
48. Matsen M. Journal of Chemical Physics 2000;113(13):5539-5544.
49. Matsen M and Thompson R. Journal of Chemical Physics 1999;111(15):7139-7146.
50. Alig I, Floudas G, Avgeropoulos A, and Hadjichristidis N. Macromolecules 1997;30(17):5004-5011.
51. Watanabe H. Macromolecules 1995;28(14):5006-5011.
52. Karatasos K, Anastasiadis S, Pakula T, and Watanabe H. Macromolecules 2000;33(2):523-541.
53. Floudas G, Paraskeva S, Hadjichristidis N, Fytas G, Chu B, and Semenov A. The Journal of chemical physics 1997;107(14):5502-5509.
54. Wu L, Lodge TP, and Bates FS. Macromolecules 2004;37(22):8184-8187.
55. Kipnusu WK, Elmahdy MM, Mapesa EU, Zhang J, Böhlmann W, Smilgies D-M, Papadakis CM, and Kremer F. ACS Applied Materials & Interfaces 2015;7(23):12328-12338.
56. Kipnusu WK, Elmahdy MM, Tress M, Fuchs M, Mapesa EU, Smilgies D-M, Zhang J, Papadakis CM, and Kremer F. Macromolecules 2013;46(24):9729-9737.
57. Wu S. Polymer Engineering and Science 1992;32(12):823-830.
58. Bero C and Roland C. Macromolecules 1996;29(5):1562-1568.
59. Khandpur AK, Förster S, Bates FS, Hamley IW, Ryan AJ, Bras W, Almdal K, and Mortensen K. Macromolecules 1995;28(26):8796-8806.
60. Georgopanos P, Rangou S, Haenelt TG, Abetz C, Meyer A, Filiz V, Handge UA, and Abetz V. Colloid and Polymer Science 2014;292(8):1877-1891.
61. Bicerano J. Prediction of Polymer Properties: CRC Press, 2002.
62. Van Krevelen DW and Te Nijenhuis K. Properties of Polymers: their correlation with chemical structure; their numerical estimation and prediction from additive group contributions: Elsevier, 2009.
63. Brandrup J, Immergut E, and Grulke E. Polymer Handbook. New York, USA: Wiley, 1999.
64. Hahn T, Shmueli U, Wilson AAJC, and Prince E. International Tables for Crystallography: D. Reidel Publishing Company, 2005.
65. Hamley IW and Castelletto V. Progress in Polymer Science 2004;29(9):909-948.
66. Matsen MW. Journal of Chemical Physics 2000;113(13):5539.
67. Haenelt TG, Georgopanos P, Abetz C, Rangou S, Alisch D, Meyer A, Handge UA, and Abetz V. Korea-Australia Rheology Journal 2014;26(3):263-275.
68. LSSHIFT Version 1.2 SGSDP, Freiburg Materials Research Center, Freiburg, Germany, Ref.:, Honerkamp J, and Weese J. Rheologica acta 1993;32(1):57-64.
69. Rouse Jr PE. The Journal of Chemical Physics 1953;21(7):1272-1280.
70. de Gennes PG. Physics Today 1983;36(6):33-39.
71. Ferry JD. Viscoelastic Properties of Polymers, 3rd ed. New York: Wiley, 1980.
72. Larson RG. The Structure and Rheology of Complex Fluids: Oxford university press New York, 1999.
73. Alig I, Kremer F, Fytas G, and Roovers J. Macromolecules 1992;25(20):5277-5282.
74. Stühn B and Stickel F. Macromolecules 1992;25(20):5306-5312.
75. Koch M, Sommer J-U, and Blumen A. The Journal of chemical physics 1997;106(3):1248-1256.
76. Yao ML, Watanabe H, Adachi K, and Kotaka T. Macromolecules 1991;24(10):2955-2962.
77. Havriliak S and Negami S. Polymer 1967;8:161-210.
78. Strobl GR. The Physics of Polymers. Berlin: Springer, 2007.

79. Boese D and Kremer F. Macromolecules 1990;23(3):829-835.